

1

Semiconductors and heterostructures

1.1 The mechanics of waves

De Broglie (see reference [1]) stated that a particle of momentum p has an associated wave of wavelength λ given by:

$$\lambda = \frac{h}{p} \quad (1.1)$$

Thus, an electron in a vacuum at a position \mathbf{r} and away from the influence of any electromagnetic potentials could be described by a *state function*, which is of the form of a wave, i.e.

$$\psi = e^{i(\mathbf{k} \cdot \mathbf{r} - \omega t)} \quad (1.2)$$

where t is the time, ω the angular frequency and the modulus of the wave vector is given by:

$$k = |\mathbf{k}| = \frac{2\pi}{\lambda} \quad (1.3)$$

The quantum mechanical momentum has been deduced to be a linear operator [2] acting upon the *wave function* ψ , with the momentum \mathbf{p} arising as an eigenvalue, i.e.

$$-i\hbar\nabla\psi = \mathbf{p}\psi \quad (1.4)$$

where

$$\nabla = \frac{\partial}{\partial x}\hat{\mathbf{i}} + \frac{\partial}{\partial y}\hat{\mathbf{j}} + \frac{\partial}{\partial z}\hat{\mathbf{k}} \quad (1.5)$$

which, when operating on the electron vacuum wave function in equation (1.2), would give the following:

$$-i\hbar\nabla e^{i(\mathbf{k} \cdot \mathbf{r} - \omega t)} = \mathbf{p}e^{i(\mathbf{k} \cdot \mathbf{r} - \omega t)} \quad (1.6)$$

and therefore

$$-i\hbar \left(\frac{\partial}{\partial x}\hat{\mathbf{i}} + \frac{\partial}{\partial y}\hat{\mathbf{j}} + \frac{\partial}{\partial z}\hat{\mathbf{k}} \right) e^{i(k_x x + k_y y + k_z z - \omega t)} = \mathbf{p}e^{i(\mathbf{k} \cdot \mathbf{r} - \omega t)} \quad (1.7)$$

Quantum Wells, Wires and Dots: Theoretical and Computational Physics of Semiconductor Nanostructures, Fourth Edition.

Paul Harrison and Alex Valavanis.

© 2016 John Wiley & Sons, Ltd. Published 2016 by John Wiley & Sons, Ltd.

$$\therefore -i\hbar \left(ik_x \hat{\mathbf{i}} + ik_y \hat{\mathbf{j}} + ik_z \hat{\mathbf{k}} \right) e^{i(k_x x + k_y y + k_z z - \omega t)} = \mathbf{p} e^{i(\mathbf{k} \cdot \mathbf{r} - \omega t)} \quad (1.8)$$

Thus the eigenvalue

$$\mathbf{p} = \hbar \left(k_x \hat{\mathbf{i}} + k_y \hat{\mathbf{j}} + k_z \hat{\mathbf{k}} \right) = \hbar \mathbf{k} \quad (1.9)$$

which, not surprisingly, can be simply manipulated ($p = \hbar k = (h/2\pi)(2\pi/\lambda)$) to reproduce de Broglie's relationship in equation (1.1).

Following on from this, classical mechanics gives the kinetic energy of a particle of mass m as:

$$T = \frac{1}{2} m v^2 = \frac{(m v)^2}{2m} = \frac{p^2}{2m} \quad (1.10)$$

Therefore it may be expected that the quantum mechanical analogy can also be represented by an eigenvalue equation with an operator:

$$\frac{1}{2m} (-i\hbar \nabla)^2 \psi = T \psi \quad (1.11)$$

i.e.

$$-\frac{\hbar^2}{2m} \nabla^2 \psi = T \psi \quad (1.12)$$

where T is the kinetic energy eigenvalue, and, given the form of ∇ in equation (1.5), then:

$$\nabla^2 = \frac{\partial^2}{\partial x^2} + \frac{\partial^2}{\partial y^2} + \frac{\partial^2}{\partial z^2} \quad (1.13)$$

When acting upon the electron vacuum wave function, i.e.

$$-\frac{\hbar^2}{2m} \nabla^2 e^{i(\mathbf{k} \cdot \mathbf{r} - \omega t)} = T e^{i(\mathbf{k} \cdot \mathbf{r} - \omega t)} \quad (1.14)$$

then

$$-\frac{\hbar^2}{2m} (i^2 k_x^2 + i^2 k_y^2 + i^2 k_z^2) e^{i(\mathbf{k} \cdot \mathbf{r} - \omega t)} = T e^{i(\mathbf{k} \cdot \mathbf{r} - \omega t)} \quad (1.15)$$

Thus the kinetic energy eigenvalue is given by:

$$T = \frac{\hbar^2 k^2}{2m} \quad (1.16)$$

For an electron in a vacuum away from the influence of electromagnetic fields, the total energy E is just the kinetic energy T . Thus the dispersion or energy versus momentum (which is proportional to the wave vector k) curves are parabolic, just as for classical free particles, as illustrated in Fig. 1.1.

The equation describing the total energy of a particle in this wave description is called the time-independent Schrödinger equation and, for this case with only a kinetic energy contribution, can be summarised as follows:

$$-\frac{\hbar^2}{2m} \nabla^2 \psi = E \psi \quad (1.17)$$

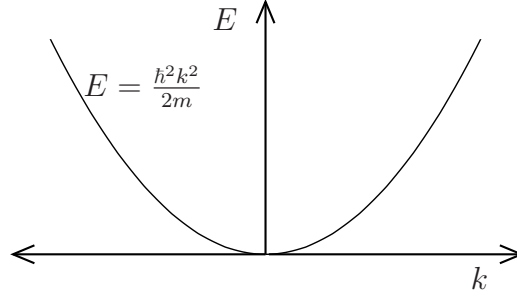


Figure 1.1: The energy versus wave vector (proportional to momentum) curve for an electron in a vacuum

A corresponding equation also exists that includes the time dependency explicitly; this is obtained by operating on the wave function by the linear operator $i\hbar\partial/\partial t$, i.e.

$$i\hbar\frac{\partial}{\partial t}e^{i(\mathbf{k}\cdot\mathbf{r}-\omega t)} = i\hbar(-i\omega)e^{i(\mathbf{k}\cdot\mathbf{r}-\omega t)} \quad (1.18)$$

or

$$i\hbar\frac{\partial}{\partial t}\psi = \hbar\omega\psi \quad (1.19)$$

Clearly, this eigenvalue $\hbar\omega$ is also the total energy but in a form usually associated with waves, e.g. a photon. These two operations on the wave function represent the two complementary descriptions associated with *wave-particle duality*. Thus the second, i.e. time-dependent, Schrödinger equation is given by:

$$i\hbar\frac{\partial}{\partial t}\psi = E\psi \quad (1.20)$$

1.2 Crystal structure

The vast majority of the mainstream semiconductors have a face-centred cubic Bravais lattice, as illustrated in Fig 1.2. The lattice points are defined in terms of linear combinations of a set of *primitive lattice vectors*, one choice for which is:

$$\mathbf{a}_1 = \frac{A_0}{2}(\hat{\mathbf{j}} + \hat{\mathbf{k}}), \quad \mathbf{a}_2 = \frac{A_0}{2}(\hat{\mathbf{k}} + \hat{\mathbf{i}}), \quad \mathbf{a}_3 = \frac{A_0}{2}(\hat{\mathbf{i}} + \hat{\mathbf{j}}) \quad (1.21)$$

The *lattice vectors* then follow as the set of vectors:

$$\mathbf{R} = \alpha_1\mathbf{a}_1 + \alpha_2\mathbf{a}_2 + \alpha_3\mathbf{a}_3 \quad (1.22)$$

where α_1 , α_2 , and α_3 are integers.

The complete crystal structure is obtained by placing the atomic basis at each Bravais lattice point. For materials such as Si, Ge, GaAs, AlAs and InP, this consists of two atoms, one at $(\frac{1}{8}, \frac{1}{8}, \frac{1}{8})$ and the other at $(-\frac{1}{8}, -\frac{1}{8}, -\frac{1}{8})$, in units of A_0 .

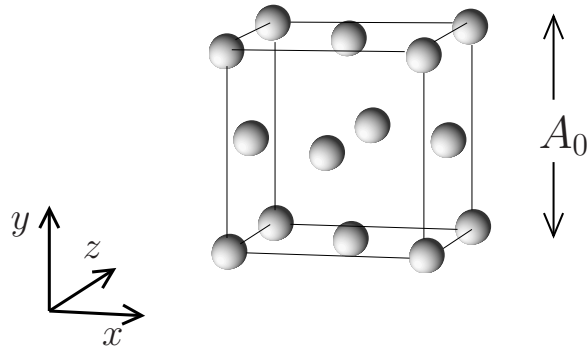


Figure 1.2: The face-centred cubic Bravais lattice

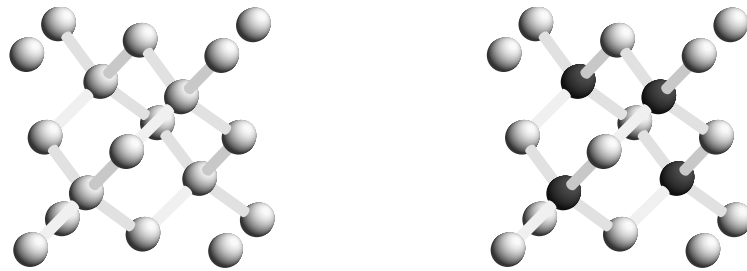


Figure 1.3: The diamond (left) and zinc blende (right) crystal structures

For the group IV materials, such as Si and Ge, as the atoms within the basis are the same, the crystal structure is equivalent to diamond (see Fig. 1.3 (left)). For III–V and II–VI compound semiconductors such as GaAs, AlAs, InP, HgTe and CdTe, the cation sits on the $(-\frac{1}{8}, -\frac{1}{8}, -\frac{1}{8})$ site and the anion on $(+\frac{1}{8}, +\frac{1}{8}, +\frac{1}{8})$; this type of crystal is called the *zinc blende* structure, after ZnS (see Fig. 1.3 (right)). The only exception to this rule is GaN, and its important $\text{In}_x\text{Ga}_{1-x}\text{N}$ alloys, which have risen to prominence in recent years due to their use in green and blue light emitting diodes and lasers (see, for example, [3]); these materials have the *wurtzite* structure (see [4], p. 47).

From an electrostatics viewpoint, the crystal potential consists of a three-dimensional lattice of spherically symmetric ionic core potentials screened by the inner shell electrons (see Fig. 1.4), which are further surrounded by the covalent bond charge distributions that hold everything together.

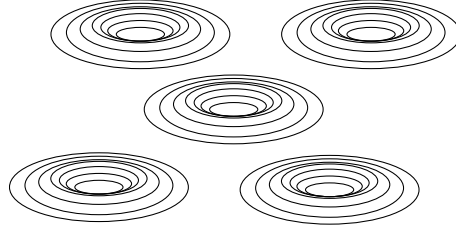


Figure 1.4: Schematic illustration of the ionic core component of the crystal potential across the $\{001\}$ planes—a three-dimensional array of spherically symmetric potentials

1.3 The effective mass approximation

Therefore, the crystal potential is complicated; however, using the principle of simplicity,¹ imagine that it can be approximated by a constant! Then the Schrödinger equation derived for an electron in a vacuum would be applicable. Clearly, though, a crystal is not a vacuum so allow the introduction of an empirical fitting parameter called the effective mass, m^* . Thus the time-independent Schrödinger equation becomes:

$$-\frac{\hbar^2}{2m^*}\nabla^2\psi = E\psi \quad (1.23)$$

and the energy solutions follow as:

$$E = \frac{\hbar^2 k^2}{2m^*} \quad (1.24)$$

This is known as the *effective mass approximation* and has been found to be very suitable for relatively low electron momenta as occur with low electric fields. Indeed, it is the most widely used parameterisation in semiconductor physics (see any good solid state physics book, e.g. [4, 5, 6]). Experimental measurements of the effective mass have revealed it to be anisotropic—as might be expected since the crystal potential along, say, the $[001]$ axis is different than along the $[111]$ axis. Adachi [7] collates reported values for GaAs and its alloys; the effective mass in other materials can be found in Landolt and Börnstein [8].

In GaAs, the reported effective mass is around $0.067 m_0$, where m_0 is the rest mass of an electron. Figure 1.5 plots the dispersion curve for this effective mass, in comparison with that of an electron in a vacuum.

1.4 Band theory

It has also been found from experiment that there are two distinct energy *bands* within semiconductors. The lower band is almost full of electrons and can conduct by the movement of the empty states. This band originates from the valence electron states which constitute the covalent bonds holding the atoms together in the crystal. In many ways, electric charge in a solid resembles a fluid, and the analogy for this band, labelled the *valence band*, is that the empty states behave like bubbles within the fluid—hence their name, *holes*.

¹Choose the simplest thing first; if it works, use it, and if it doesn't, then try the next simplest!

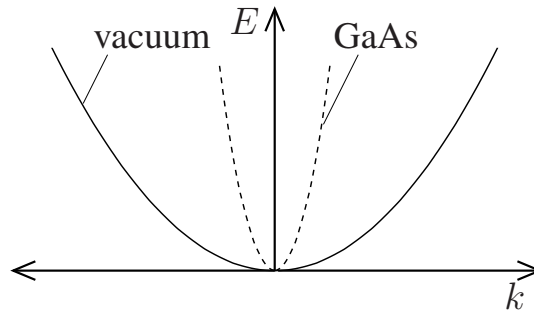


Figure 1.5: The energy versus wave vector (proportional to momentum) curves for an electron in GaAs compared to that in a vacuum

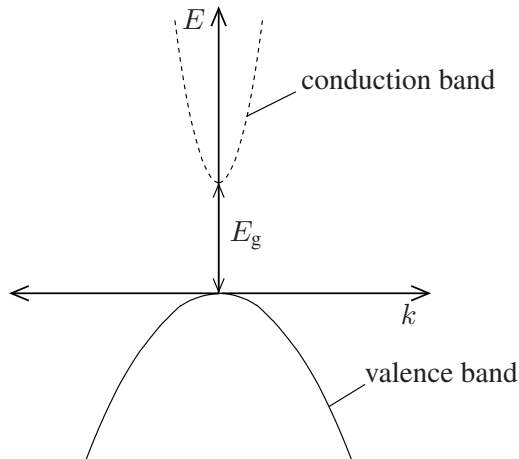


Figure 1.6: The energy versus wave vector curves for an electron in the conduction band and a hole in the valence band of GaAs

In particular, the holes rise to the uppermost point of the valence band, and just as it is possible to consider the release of carbon dioxide through the motion of beer in a glass, it is actually easier to study the motion of the bubble (the absence of beer), or in this case the motion of the hole.

In a semiconductor, the upper band is almost devoid of electrons. It represents excited electron states which are occupied by electrons promoted from localised covalent bonds into extended states in the body of the crystal. Such electrons are readily accelerated by an applied electric field and contribute to current flow. This band is therefore known as the *conduction band*.

Figure 1.6 illustrates these two bands. Notice how the valence band is inverted—this is a reflection of the fact that the ‘bubbles’ rise to the top, i.e. their lowest-energy states are at

the top of the band. The energy difference between the two bands is known as the *band gap*, labelled as E_{gap} on the figure. The particular curvatures used in both bands are indicative of those measured experimentally for GaAs, namely effective masses of around $0.067 m_0$ for an electron in the conduction band, and $0.6 m_0$ for a (heavy) hole in the valence band. The convention is to put the zero of the energy at the top of the valence band. Note the extra qualifier ‘heavy’. In fact, there is more than one valence band, and they are distinguished by their different effective masses. Chapter 15 will discuss band structure in more detail; this will be in the context of a microscopic model of the crystal potential which goes beyond the simple ideas introduced here.

1.5 Heterojunctions

The effective mass approximation is for a bulk crystal, which means the crystal is so large with respect to the scale of an electron wave function that it is effectively infinite. Within the effective mass approximation, the Schrödinger equation has been found to be as follows:

$$-\frac{\hbar^2}{2m^*} \frac{\partial^2}{\partial z^2} \psi(z) = E\psi(z) \quad (1.25)$$

When two such materials are placed adjacent to each other to form a *heterojunction*, this equation is valid within each, remembering of course that the effective mass could be a function of position. However, the band gaps of the materials can also be different (see Fig. 1.7).

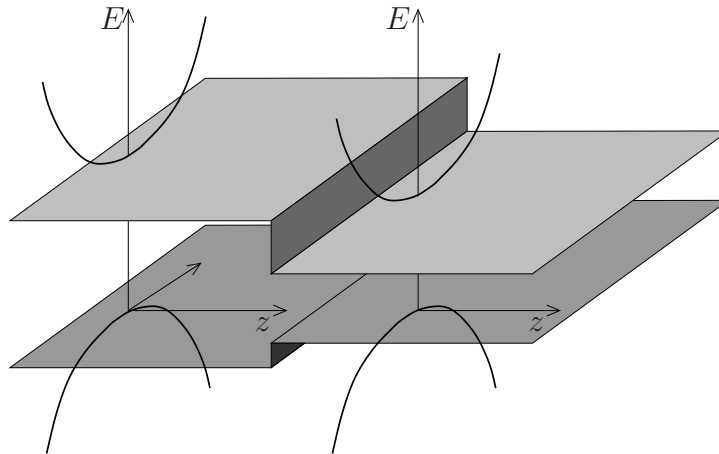


Figure 1.7: Two dissimilar semiconductors with different band gaps joined to form a heterojunction; the curves represent the unrestricted motion parallel to the interface

The discontinuity in either the conduction or the valence band can be represented by a constant potential term. Thus the Schrödinger equation for any one of the bands, taking the

effective mass to be the same in each material, would be generalised to:

$$-\frac{\hbar^2}{2m^*} \frac{\partial^2}{\partial z^2} \psi(z) + V(z)\psi(z) = E\psi(z) \quad (1.26)$$

In the above example, the one-dimensional potentials $V(z)$ representing the band discontinuities at the heterojunction would have the form shown in Fig. 1.8, noting that increasing hole energy in the valence band is measured downwards.

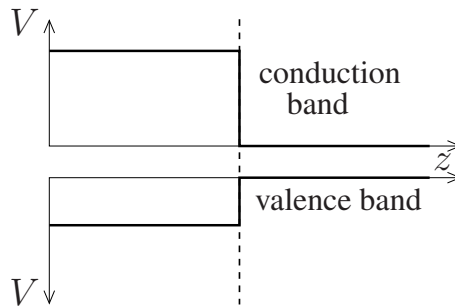


Figure 1.8: The one-dimensional potentials $V(z)$ in the conduction and valence band as might occur at a heterojunction (marked with a dashed line) between two dissimilar materials

1.6 Heterostructures

Heterostructures are formed from multiple heterojunctions, and thus a myriad of possibilities exist. If a thin layer of a narrower-bandgap material (A, say) is sandwiched between two layers of a wider-bandgap material (B), as illustrated in Fig. 1.9 (left), then they form a double heterojunction. If layer A is sufficiently thin for *quantum properties* to be exhibited, then such a band alignment is called a *single quantum well*.

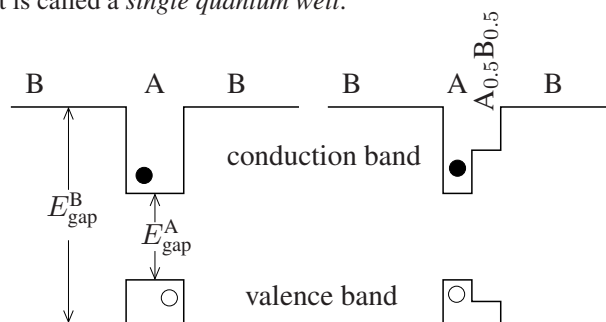


Figure 1.9: The one-dimensional potentials $V(z)$ in the conduction and valence bands for a typical single quantum well (left) and a stepped quantum well (right)

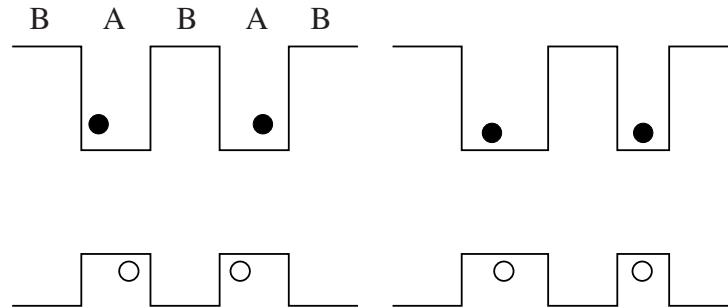


Figure 1.10: The one-dimensional potentials $V(z)$ in the conduction and valence band for typical *symmetric* (left) and *asymmetric* (right) double quantum wells

If any charge carriers exist in the system, whether thermally produced intrinsic or extrinsic as the result of doping, they will attempt to lower their energies. Hence in this example, any electrons (solid circles) or holes (open circles) will collect in the quantum well (see Fig. 1.9). Additional semiconductor layers can be included in the heterostructure, for example a *stepped* or *asymmetric* quantum well can be formed by the inclusion of an alloy between materials A and B, as shown in Fig. 1.9 (right).

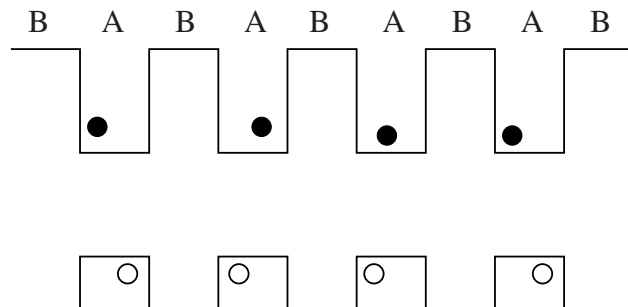


Figure 1.11: The one-dimensional potentials $V(z)$ in the conduction and valence band for a typical multiple quantum well or superlattice

Still more complex structures can be formed, such as symmetric or asymmetric *double quantum wells*, (see Fig. 1.10) and *multiple quantum wells* or *superlattices* (see Fig. 1.11). The difference between the latter is the extent of the interaction between the quantum wells; in particular, a multiple quantum well exhibits the properties of a collection of isolated single quantum wells, whereas in a superlattice the quantum wells do interact. The motivation behind introducing increasingly complicated structures is an attempt to tailor the electronic and optical properties of these materials for exploitation in devices. Perhaps the most complicated layer structure to date is the *chirped superlattice* active region of a mid-infrared laser [9].

All of the structures illustrated so far have been examples of Type-I systems. In this type, the band gap of one material is nestled entirely within that of the wider-bandgap material. The consequence of this is that any electrons or holes fall into quantum wells which are *within* the same layer of material. Thus both types of charge carrier are localised in the same region of space, which makes for efficient (fast) recombination. However, other possibilities can exist, as illustrated in Fig. 1.12.

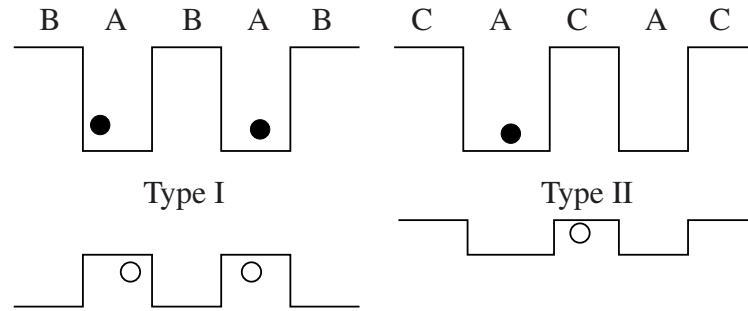


Figure 1.12: The one-dimensional potentials $V(z)$ in the conduction and valence bands for a typical Type-I superlattice (left) compared to a Type-II system (right)

In Type-II systems the band gaps of the materials (say, A and C) are aligned such that the quantum wells formed in the conduction and valence bands are in different materials, as illustrated in Fig. 1.12 (right). This leads to the electrons and holes being confined in *different* layers of the semiconductor. The consequence of this is that the recombination times of electrons and holes are long.

1.7 The envelope function approximation

Two important points have been argued:

1. The effective mass approximation *is* a valid description of bulk materials.
2. Heterojunctions between dissimilar materials, both of which can be well represented by the effective mass approximation, can be described by a material potential which derives from the difference in the band gaps.

The logical extension to point 2 is that the crystal potential of multiple heterojunctions can also be described in this manner, as illustrated extensively in the previous section.

Once this is accepted, then the electronic structure *can* be represented by the simple one-dimensional Schrödinger equation that has been aspired to:

$$-\frac{\hbar^2}{2m^*} \frac{\partial^2}{\partial z^2} \psi(z) + V(z)\psi(z) = E\psi(z) \quad (1.27)$$

The *envelope function approximation* is the name given to the mathematical justification for this series of arguments (see, for example, works by Bastard [10, 11] and Burt [12, 13]).

The name derives from the deduction that physical properties can be derived from the slowly varying envelope function, identified here as $\psi(z)$, rather than the total wave function $\psi(z)u(z)$, where the latter is rapidly varying on the scale of the crystal lattice. The validity of the envelope function approximation is still an active area of research [13]. With the line of reasoning used here, it is clear that the envelope function approximation *can* be thought of as an approximation on the material and *not* the quantum mechanics.

Some thought is enough to appreciate that the envelope function approximation will have limitations, and that these will occur for very thin layers of material. The materials *are* made of a collection of a large number of atomic potentials, so when a layer becomes thin, these individual potentials will become significant and the global average of representing the crystal potential by a constant will breakdown (see, for example, [14]). However, for the majority of examples this approach works well; this will be demonstrated in later chapters, and, in particular, a detailed comparison with an alternative approach which does account fully for the microscopic crystal potential will be made in Chapter 16.

1.8 Band non-parabolicity

For semiconductor heterostructures with relatively low barrier heights and low carrier densities, the carriers cluster at energies near the conduction-band edge, i.e. within a couple of hundred millielectronvolts, compared to a band gap of the order of 1.5 eV. In this region, the band edge can be described by a parabolic E - k curve, i.e. in the form given by equation (1.24).

However, in situations where the carriers are forced up to higher energies, either by large barrier heights and narrow wells (as discussed in Chapter 2), or by very high carrier densities or high temperatures, equation (1.24) is only an approximate description of the carrier dispersion. This is especially important for holes in the valence band. The approximation can be improved upon by adding summation terms into the polynomial expansion for the energy. For example, no matter how complex the band structure along a particular direction, it clearly has inversion symmetry and hence can always be represented by an expansion in even powers of k , if sufficient terms are included, i.e. the energy E can be described by:

$$E = a_0k^0 + a_2k^2 + a_4k^4 + a_6k^6 + a_8k^8 + \dots = \sum_{i=0}^{\infty} a_{2i}k^{2i} \quad (1.28)$$

Usually when discussing single band models, as has been focused on entirely so far, the energy origin is set at the bottom of the band of interest, and thus $a_0 = 0$. In addition, truncating the series at k^2 gives $a_2 = \hbar^2/(2m^*)$.

The next best approximation is to include terms in k^4 , hence accounting for band non-parabolicity, as displayed in Fig. 1.13, with:

$$E = a_2k^2 + a_4k^4 = \frac{\hbar^2}{2m^*} (k^2 + \beta k^4) \quad (1.29)$$

where

$$\beta = a_2 \frac{2m^*}{\hbar^2} \quad (1.30)$$

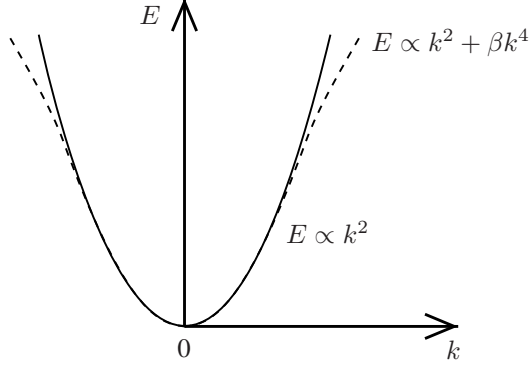


Figure 1.13: Dispersion relations for parabolic (solid line) and non-parabolic band (dashed line) models

Using the basic definition of effective mass, i.e.

$$m^* = \hbar^2 \left(\frac{\partial^2 E}{\partial k^2} \right)^{-1} \quad (1.31)$$

then clearly m^* remains a function of k , unlike the case of parabolic bands where it is a constant. As it is a function of k , then it is also a function of energy, and indeed band non-parabolicity is accounted for by an energy-dependent effective mass [15]:

$$m^*(E) = m^*(0)[1 + \alpha(E - V)] \quad (1.32)$$

where V is the band-edge potential.

The non-parabolicity parameter, α , is usually greatest when the band edge under consideration is close to other energy bands in the material. Precise values of α may be obtained experimentally or extracted from more detailed models of the band structure, such as those considered in Chapters 14 and 16. However, simple approximations exist near the edge of the conduction band, such as that given by [16, 17]:

$$\alpha = \left[1 - \frac{m^*(0)}{m_0} \right]^2 / E_g \quad (1.33)$$

where E_g is the semiconductor band gap, or the even simpler model given by [18, 19]:

$$\alpha = 1/E_g \quad (1.34)$$

The latter expression can be used to estimate the significance of non-parabolicity in a range of different materials. In GaAs, for example, $E_g = 1.426$ eV, giving $\alpha = 0.701$ eV⁻¹. The effective mass of an electron 100 meV above the conduction-band edge in GaAs, therefore, has an effective mass 7% higher than that at the band edge. By comparison, in InSb, $E_g = 0.18$ eV and $\alpha = 5.6$ eV⁻¹, meaning that an equivalent electron has an effective mass 56% higher than that at the band edge. This illustrates that although non-parabolicity may be

very significant in narrow-bandgap semiconductors, it can be ignored safely for low-energy electrons in many common materials.

For this reason, non-parabolicity is neglected throughout most of this book, and the focus is placed on the much more elegant and immediately intuitive models of the behaviour of carriers with parabolic dispersion. However, Chapter 2 illustrates how non-parabolicity affects analytical models of certain phenomena, and Chapter 3 describes how it may be included in numerical methods.

1.9 The reciprocal lattice

For later discussions the concept of the *reciprocal lattice* needs to be developed. It has already been shown that considering electron wave functions as plane waves ($e^{i\mathbf{k}\cdot\mathbf{r}}$), as found in a vacuum, but with a correction factor called the effective mass, is a useful method of approximating the electronic band structure. In general, such a wave will not have the periodicity of the crystal lattice; however, for certain wave vectors it will. Such a set of wave vectors \mathbf{G} are known as the *reciprocal lattice vectors* with the set of points mapped out by these primitives known as the *reciprocal lattice*.

If the set of vectors \mathbf{G} *did* have the periodicity of the lattice, then this would imply that:

$$e^{i\mathbf{G}\cdot(\mathbf{r}+\mathbf{R})} = e^{i\mathbf{G}\cdot\mathbf{r}} \quad (1.35)$$

i.e. an electron with this wave vector \mathbf{G} would have a wave function equal at all points in real space separated by a Bravais lattice vector \mathbf{R} . Therefore:

$$e^{i\mathbf{G}\cdot\mathbf{r}} e^{i\mathbf{G}\cdot\mathbf{R}} = e^{i\mathbf{G}\cdot\mathbf{r}} \quad (1.36)$$

which implies that

$$\mathbf{G}\cdot\mathbf{R} = 2\pi n, \quad n \in \mathbb{Z} \quad (1.37)$$

Now learning from the form for the Bravais lattice vectors \mathbf{R} given earlier in equation (1.22), it might be expected that the reciprocal lattice vectors \mathbf{G} could be constructed in a similar manner from a set of three *primitive reciprocal lattice vectors*, i.e.

$$\mathbf{G} = \beta_1 \mathbf{b}_1 + \beta_2 \mathbf{b}_2 + \beta_3 \mathbf{b}_3, \quad \beta_1, \beta_2, \beta_3 \in \mathbb{Z} \quad (1.38)$$

With these choices, then, the primitive reciprocal lattice vectors can be written as follows:

$$\mathbf{b}_1 = 2\pi \frac{\mathbf{a}_2 \times \mathbf{a}_3}{\mathbf{a}_1 \cdot (\mathbf{a}_2 \times \mathbf{a}_3)} \quad (1.39)$$

$$\mathbf{b}_2 = 2\pi \frac{\mathbf{a}_3 \times \mathbf{a}_1}{\mathbf{a}_1 \cdot (\mathbf{a}_2 \times \mathbf{a}_3)} \quad (1.40)$$

$$\mathbf{b}_3 = 2\pi \frac{\mathbf{a}_1 \times \mathbf{a}_2}{\mathbf{a}_1 \cdot (\mathbf{a}_2 \times \mathbf{a}_3)} \quad (1.41)$$

It is possible to verify that these forms do satisfy equation (1.37):

$$\mathbf{G}\cdot\mathbf{R} = (\beta_1 \mathbf{b}_1 + \beta_2 \mathbf{b}_2 + \beta_3 \mathbf{b}_3) \cdot (\alpha_1 \mathbf{a}_1 + \alpha_2 \mathbf{a}_2 + \alpha_3 \mathbf{a}_3) \quad (1.42)$$

Now \mathbf{b}_1 is perpendicular to both \mathbf{a}_2 and \mathbf{a}_3 , and so only the product of \mathbf{b}_1 with \mathbf{a}_1 is non-zero, and similarly for \mathbf{b}_2 and \mathbf{b}_3 . Hence:

$$\mathbf{G} \cdot \mathbf{R} = \beta_1 \alpha_1 \mathbf{b}_1 \cdot \mathbf{a}_1 + \beta_2 \alpha_2 \mathbf{b}_2 \cdot \mathbf{a}_2 + \beta_3 \alpha_3 \mathbf{b}_3 \cdot \mathbf{a}_3 \quad (1.43)$$

and in fact, the products $\mathbf{b}_i \cdot \mathbf{a}_i = 2\pi$. Therefore:

$$\mathbf{G} \cdot \mathbf{R} = 2\pi (\beta_1 \alpha_1 + \beta_2 \alpha_2 + \beta_3 \alpha_3) \quad (1.44)$$

Clearly $\beta_1 \alpha_1 + \beta_2 \alpha_2 + \beta_3 \alpha_3$ is an integer, and hence equation (1.37) is satisfied.

Using the face-centred cubic lattice vectors defined in equation (1.21), then:

$$\mathbf{a}_1 \cdot (\mathbf{a}_2 \times \mathbf{a}_3) = \begin{vmatrix} a_{1x} & a_{1y} & a_{1z} \\ a_{2x} & a_{2y} & a_{2z} \\ a_{3x} & a_{3y} & a_{3z} \end{vmatrix} = \begin{vmatrix} 0 & \frac{A_0}{2} & \frac{A_0}{2} \\ \frac{A_0}{2} & 0 & \frac{A_0}{2} \\ \frac{A_0}{2} & \frac{A_0}{2} & 0 \end{vmatrix} \quad (1.45)$$

which gives:

$$\mathbf{a}_1 \cdot (\mathbf{a}_2 \times \mathbf{a}_3) = 0 \times \begin{vmatrix} 0 & \frac{A_0}{2} \\ \frac{A_0}{2} & 0 \end{vmatrix} - \frac{A_0}{2} \begin{vmatrix} \frac{A_0}{2} & \frac{A_0}{2} \\ \frac{A_0}{2} & 0 \end{vmatrix} + \frac{A_0}{2} \begin{vmatrix} \frac{A_0}{2} & 0 \\ \frac{A_0}{2} & \frac{A_0}{2} \end{vmatrix} \quad (1.46)$$

$$\therefore \mathbf{a}_1 \cdot (\mathbf{a}_2 \times \mathbf{a}_3) = 0 - \frac{A_0}{2} \left[0 - \left(\frac{A_0}{2} \right)^2 \right] + \frac{A_0}{2} \left[\left(\frac{A_0}{2} \right)^2 - 0 \right] \quad (1.47)$$

$$\therefore \mathbf{a}_1 \cdot (\mathbf{a}_2 \times \mathbf{a}_3) = 2 \left(\frac{A_0}{2} \right)^3 \quad (1.48)$$

Therefore, the first of the primitive reciprocal lattice vectors follows as:

$$\mathbf{b}_1 = 2\pi \left[2 \left(\frac{A_0}{2} \right)^3 \right]^{-1} \begin{vmatrix} \hat{\mathbf{i}} & \hat{\mathbf{j}} & \hat{\mathbf{k}} \\ \frac{A_0}{2} & 0 & \frac{A_0}{2} \\ \frac{A_0}{2} & \frac{A_0}{2} & 0 \end{vmatrix} \quad (1.49)$$

$$\begin{aligned} \therefore \mathbf{b}_1 &= 2\pi \frac{1}{2} \left(\frac{2}{A_0} \right)^3 \\ &\times \left\{ \left[0 - \left(\frac{A_0}{2} \right)^2 \right] \hat{\mathbf{i}} - \left[0 - \left(\frac{A_0}{2} \right)^2 \right] \hat{\mathbf{j}} + \left[\left(\frac{A_0}{2} \right)^2 - 0 \right] \hat{\mathbf{k}} \right\} \end{aligned} \quad (1.50)$$

$$\therefore \mathbf{b}_1 = \frac{2\pi}{A_0} (-\hat{\mathbf{i}} + \hat{\mathbf{j}} + \hat{\mathbf{k}}) \quad (1.51)$$

A similar calculation of the remaining primitive reciprocal lattice vectors \mathbf{b}_2 and \mathbf{b}_3 gives the complete set as follows:

$$\mathbf{b}_1 = \frac{2\pi}{A_0} (-\hat{\mathbf{i}} + \hat{\mathbf{j}} + \hat{\mathbf{k}}), \quad \mathbf{b}_2 = \frac{2\pi}{A_0} (\hat{\mathbf{i}} - \hat{\mathbf{j}} + \hat{\mathbf{k}}), \quad \mathbf{b}_3 = \frac{2\pi}{A_0} (\hat{\mathbf{i}} + \hat{\mathbf{j}} - \hat{\mathbf{k}}) \quad (1.52)$$

which are, of course, equivalent to the body-centred cubic Bravais lattice vectors (see [5], p. 68). Thus the reciprocal lattice constructed from the linear combinations:

$$\mathbf{G} = \beta_1 \mathbf{b}_1 + \beta_2 \mathbf{b}_2 + \beta_3 \mathbf{b}_3, \quad \beta_1, \beta_2, \beta_3 \in \mathbb{Z} \quad (1.53)$$

Table 1.1 Generation of the reciprocal lattice vectors for the face-centred cubic crystal by the systematic selection of the integer coefficients β_1 , β_2 and β_3

β_1	β_2	β_3	Reciprocal lattice vector, \mathbf{G} ($2\pi/A_0$)
0	0	0	(0, 0, 0)
1	0	0	($\bar{1}$, 1, 1)
0	1	0	(1, $\bar{1}$, 1)
0	0	1	(1, 1, $\bar{1}$)
-1	0	0	(1, $\bar{1}$, $\bar{1}$)
0	-1	0	($\bar{1}$, 1, $\bar{1}$)
0	0	-1	($\bar{1}$, $\bar{1}$, 1)
1	1	1	(1, 1, 1)
-1	-1	-1	($\bar{1}$, $\bar{1}$, $\bar{1}$)
1	1	0	(0, 0, 2)
1	0	1	(0, 2, 0)
0	1	1	(2, 0, 0)
-1	1	0	(2, $\bar{2}$, 2)
(etc.)			

is a body-centred cubic lattice with lattice constant $4\pi/A_0$.

Taking the face-centred cubic primitive reciprocal lattice vectors in equation (1.52), then:

$$\mathbf{G} = \frac{2\pi}{A_0} [\beta_1(-\hat{\mathbf{i}} + \hat{\mathbf{j}} + \hat{\mathbf{k}}) + \beta_2(\hat{\mathbf{i}} - \hat{\mathbf{j}} + \hat{\mathbf{k}}) + \beta_3(\hat{\mathbf{i}} + \hat{\mathbf{j}} - \hat{\mathbf{k}})] \quad (1.54)$$

$$\therefore \mathbf{G} = \frac{2\pi}{A_0} [(-\beta_1 + \beta_2 + \beta_3)\hat{\mathbf{i}} + (\beta_1 - \beta_2 + \beta_3)\hat{\mathbf{j}} + (\beta_1 + \beta_2 - \beta_3)\hat{\mathbf{k}}] \quad (1.55)$$

The specific reciprocal lattice vectors are therefore generated by taking different combinations of the integers β_1 , β_2 , and β_3 . This is illustrated in Table 1.1.

It was shown by von Laue that, when waves in a periodic structure satisfied the following:

$$\mathbf{k} \cdot \hat{\mathbf{G}} = \frac{1}{2} |\mathbf{G}| \quad (1.56)$$

diffraction would occur (see [5], p. 99). Thus the ‘free’ electron dispersion curves of earlier (Fig. 1.5), will be perturbed when the electron wave vector satisfies equation (1.56). Along the [001] direction, the smallest reciprocal lattice vector \mathbf{G} is (0,0,2) (in units of $2\pi/A_0$). Substituting into equation (1.56) gives:

$$\mathbf{k} \cdot (0\hat{\mathbf{i}} + 0\hat{\mathbf{j}} + \hat{\mathbf{k}}) = \frac{1}{2} \times 2 \times \frac{2\pi}{A_0} \quad (1.57)$$

This then implies the electron will be diffracted when:

$$\mathbf{k} = \frac{2\pi}{A_0} \hat{\mathbf{k}} \quad (1.58)$$

Figure 1.14 illustrates the effect that such diffraction would have on the ‘free electron’ curves. At wave vectors which satisfy von Laue’s condition, the energy bands are disturbed

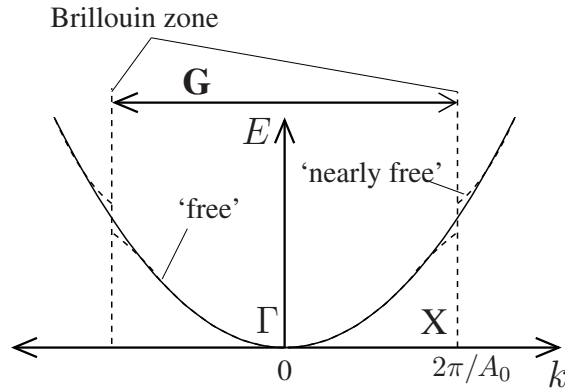


Figure 1.14: Comparison of the free and nearly free electron models

and an energy gap opens. Such an improvement on the parabolic dispersion curves of earlier is known as the *nearly free electron model*.

The space between the lowest wave vector solutions to von Laue's condition is called the first *Brillouin zone*. Note that the reciprocal lattice vectors in any particular direction span the Brillouin zone. As mentioned above, a face-centred cubic lattice has a body-centred cubic reciprocal lattice, and therefore the Brillouin zone is a three-dimensional solid, which happens to be a 'truncated octahedron' (see, for example, [5], p. 89). High-symmetry points around the Brillouin zone are often labelled for ease of reference, with the most important of these, for this work, being the $k = 0$ point, referred to as ' Γ ', and the $\langle 001 \rangle$ zone edges, which are called the ' X ' points.

Exercises

All necessary material parameters are given in Appendix A.

- (1). Consider a free electron with a velocity of $2 \times 10^5 \text{ m s}^{-1}$ in the z -direction.
 - (a) Calculate the de Broglie wavelength and wave vector of the electron.
 - (b) Assuming a wave function with the form $\psi(\mathbf{r}, t) = A \exp[i(\mathbf{k} \cdot \mathbf{r} - \omega t)]$, where A is a constant, determine the kinetic energy of the electron using equation (1.17).
 - (c) Confirm that the result is in agreement with the classical expression for kinetic energy, given in equation (1.10).
- (2).
 - (a) List the atomic locations that lie within a face-centred cubic unit cell of GaAs [$0 \leq (x, y, z) \leq A_0$].
 - (b) Hence, estimate the number of atoms in a cube of GaAs with $1 \mu\text{m}^3$ volume.
 - (c) Taking the molar mass of a GaAs molecule as $144.645 \text{ g mol}^{-1}$ and Avogadro's number $N_A = 6.022 \times 10^{23} \text{ mol}^{-1}$, use the answer to part (b) to estimate the mass density of a GaAs crystal.

- (d) Compare the calculated density with that given in Appendix A. What conclusions may be drawn from the result?
- (3). Find the difference in energy between an electron and a heavy hole with a wave vector of $\mathbf{k} = 0.05 \Gamma\bar{X}$ in GaAs.
 - (4). Sketch the one-dimensional potential profile for the conduction- and valence-band edges in a heterostructure consisting of a 2 nm thick layer of GaAs surrounded by a pair of 10 nm thick layers of $\text{Al}_{0.15}\text{Ga}_{0.85}\text{As}$.
 - (5). The ‘L’ symmetry points for a face-centred cubic crystal lie at the $\langle 111 \rangle$ zone edges. Determine their coordinates using equation (1.56) and the results in Table 1.1.
 - (6). Most semiconductor materials take the diamond or zinc blende structure of two interlocking face-centred cubic crystal lattices. However, GaN-based semiconductors, which are being used increasingly in green and blue laser diodes, form a hexagonal, wurtzite structure. Find the primitive lattice vectors for a hexagonal Bravais lattice and the atomic basis necessary to describe GaN.

References

- [1] R. T. Weidner and R. L. Sells, *Elementary Modern Physics*, Allyn and Bacon, Boston, Third edition, 1980.
- [2] P. A. M. Dirac, *The Principles of Quantum Mechanics*, Clarendon Press, Oxford, Fourth edition, 1967.
- [3] S. Nakamura and G. Fasol, *The Blue Laser Diode*, Springer, Berlin, 1997.
- [4] J. S. Blakemore, *Solid State Physics*, Cambridge University Press, Cambridge, Second edition, 1985.
- [5] N. W. Ashcroft and N. D. Mermin, *Solid State Physics*, Saunders College Publishing, Philadelphia, 1976.
- [6] M. J. Kelly, *Low Dimensional Semiconductors: Materials, Physics, Technology, Devices*, Clarendon Press, Oxford, 1995.
- [7] S. Adachi, *GaAs and Related Materials: Bulk Semiconducting and Superlattice Properties*, World Scientific, Singapore, 1994.
- [8] H. Landolt and R. Börnstein, Eds., *Numerical Data and Functional Relationships in Science and Technology*, vol. 22a of *Series III*, Springer-Verlag, Berlin, 1987.
- [9] A. Tredicucci, C. Gmachl, F. Capasso, D. L. Sivco, and A. L. Hutchinson, ‘Long wavelength superlattice quantum cascade lasers at $\lambda \approx 17 \mu\text{m}$ ’, *Appl. Phys. Lett.*, **74**:638, 1999.
- [10] G. Bastard, ‘Superlattice band structure in the envelope-function approximation’, *Phys. Rev. B*, **24**(10):5693–5697, 1981.
- [11] G. Bastard, *Wave Mechanics Applied to Semiconductor Heterostructures*, Monographies de physique. Halsted Press, New York, 1988.
- [12] M. G. Burt, ‘The justification for applying the effective-mass approximation to microstructures’, *J. Phys.: Condens. Matter*, **4**:6651, 1992.
- [13] M. G. Burt, ‘Fundamentals of envelope function theory for electronic states and photonic modes in nanostructures’, *J. Phys.: Condens. Matter*, **11**(9):53, 1999.
- [14] F. Long, W. E. Hagston, and P. Harrison, ‘Breakdown of the envelope function/effective mass approximation in narrow quantum wells’, in *The Proceedings of the 23rd International Conference on the Physics of Semiconductors*, Singapore, 1996, pp. 1819–1822, World Scientific.
- [15] Y. Hirayama, J. H. Smet, L.-H. Peng, C. G. Fonstad, and E. P. Ippen, ‘Feasibility of 1.55 μm intersubband photonic devices using InGaAs/AlAs pseudomorphic quantum well structures’, *Jpn. J. Appl. Phys.*, **33**(1S):890, 1994.
- [16] H. Asai and Y. Kawamura, ‘Intersubband absorption in $\text{In}_{0.53}\text{Ga}_{0.47}\text{As}/\text{In}_{0.52}\text{Al}_{0.48}\text{As}$ multiple quantum wells’, *Phys. Rev. B*, **43**(6):4748–4759, 1991.
- [17] A. Raymond, J. L. Robert, and C. Bernard, ‘The electron effective mass in heavily doped GaAs’, *J. Phys. C: Solid State Phys.*, **12**(12):2289, 1979.

- [18] D. F. Nelson, R. C. Miller, and D. A. Kleinman, 'Band nonparabolicity effects in semiconductor quantum wells', *Phys. Rev. B*, **35**(14):7770–7773, 1987.
- [19] M. P. Hasselbeck and P. M. Enders, 'Electron–electron interactions in the nonparabolic conduction band of narrow-gap semiconductors', *Phys. Rev. B*, **57**(16):9674–9681, 1998.